APL Photonics

Continuous-wave Raman amplification in silicon core fibers pumped in the telecom band

Cite as: APL Photonics **6**, 096105 (2021); https://doi.org/10.1063/5.0060108
Submitted: 15 June 2021 • Accepted: 22 August 2021 • Published Online: 08 September 2021

Meng Huang, Shiyu Sun, Dong Wu, et al.

AIP Publishing

Continuous-wave Raman amplification in silicon core fibers pumped in the telecom band

Cite as: APL Photon. 6, 096105 (2021); doi: 10.1063/5.0060108
Submitted: 15 June 2021 • Accepted: 22 August 2021 •
Published Online: 8 September 2021

Meng Huang,[1] Shiyu Sun,[1] Dong Wu,[1] Haonan Ren,[1] Li Shen,[2,a)] Thomas W. Hawkins,[3] John Ballato,[3] Ursula J. Gibson,[4,b)] and Anna C. Peacock[1,a)]

AFFILIATIONS

[1] Optoelectronics Research Centre, University of Southampton, Southampton SO17 1BJ, United Kingdom
[2] Wuhan National Laboratory for Optoelectronics and School of Optical and Electrical Information, Huazhong University of Science and Technology, Wuhan 430074, China
[3] Center for Optical Materials Science and Engineering Technologies and Department of Materials Science and Engineering, Clemson University, Clemson, South Carolina 29634, USA
[4] Department of Physics and Porelabs, Norwegian University of Science and Technology, N-7491 Trondheim, Norway

[a)] **Authors to whom correspondence should be addressed:** lishen@hust.edu.cn and acp@orc.soton.ac.uk
[b)] **Also at:** Department of Applied Physics, KTH Royal Institute of Technology, Stockholm 10044, Sweden.

ABSTRACT

Stimulated Raman amplification is observed for the first time in the silicon core fiber (SCF) platform. The SCFs were tapered to obtain sub-micrometer core dimensions and low optical transmission losses, facilitating efficient spontaneous scattering and stimulated Raman amplification using a continuous-wave pump source with milliwatt power levels. A maximum on–off gain of 1.1dB was recorded at a pump power of only 48 mW with our numerical simulations, indicating that gains up to 6 dB are achievable by increasing the fiber length. This work shows that the SCF platform could open a route to producing compact and robust all-fiber integrated Raman amplifiers and lasers across a broad wavelength region.

I. INTRODUCTION

Raman scattering offers a convenient route to developing amplifiers and light sources from waveguide materials that do not possess a direct bandgap. Although much of the early research on Raman systems made use of long lengths of silica fiber,[1] more recently, the focus has shifted to silicon waveguides due to their high Raman gain coefficient and the potential to exploit such systems in compact architectures.[2–5] However, to date, the achievable gain in silicon systems within the telecom band has been hindered by the relatively high linear and nonlinear transmission losses. To reduce the linear losses, waveguides with large, micrometer-sized dimensions have been employed, but these have required the use of impractically high coupled pump powers [~1 W continuous-wave (CW)] to achieve Raman gains up to 2.3 dB due to the reduced light confinement.[6] Alternately, when using smaller, sub-micrometer waveguide dimensions, both the linear and nonlinear losses play a significant role, and thus, pulsed pump sources have been required to reduce the build-up of free carriers to obtain similar levels of gain.[7]

In recent years, an alternative silicon core fiber (SCF) platform has emerged, which combines several benefits of the fiber geometry with the highly nonlinear silicon core materials, making it well suited for the development of efficient Raman systems.[8] The SCFs are typically fabricated via the molten core drawing (MCD) method, which allows for the rapid production of long lengths of fiber, increasing the device yield and lowering production costs.[9,10] Tapering procedures are subsequently employed to obtain sub-micrometer core dimensions that are desired for efficient nonlinear processes.[11] With advancements to the fabrication techniques, the small core SCFs can be produced to exhibit low losses over centimeter lengths, opening a route to obtaining effective levels of Raman gain using modest CW pump powers. Significantly, compared to their planar counterparts, the SCFs offer several advantages for practical systems as they are robust and polarization independent, and they can be spliced directly to fiber pump lasers and networks.[12,13]

In this paper, we present the first investigations of spontaneous and stimulated Raman scattering within the tapered SCFs. The Raman gain coefficient is found to be in good agreement with

values reported for planar silicon waveguides (~30 cm/GW), providing evidence for the high crystalline quality of the processed fiber core. The combination of low transmission loss (~1 dB/cm) and centimeter long waveguide lengths has allowed for a peak gain of 1.1 dB to be achieved with a CW power of only 48 mW. Numerical simulations of the nonlinear propagation suggest that Raman gains up to 6 dB are achievable by increasing the SCF length while still keeping the power levels to ~100 mW. We anticipate that with continued efforts to reduce the transmission losses over longer lengths, these SCFs could open new possibilities for all-fiber Raman-based laser sources and amplifiers.

II. FIBER FABRICATION AND NONLINEAR PROPAGATION EQUATION

The SCFs used in this work were fabricated using the MCD method, which is based on conventional fiber drawing techniques whereby the low melting temperature semiconductor core is encapsulated in the softened silica cladding.[9] The as-drawn SCFs have a polycrystalline core material with a uniform core/cladding diameter of 12 μm/125 μm. Owing to the differences in the thermal properties of the crystalline core and glass cladding, obtaining SCFs with small core sizes straight from the drawing tower can be challenging. Thus, to enhance the nonlinear performance, the as-drawn SCFs were subsequently tapered using a two-step process to obtain fibers with sub-micrometer core diameters.[14] Compared to a single step taper process, the tapering temperature (heated by a filament) used in the two-step process is much lower, which allows for the production of continuous silicon cores with large crystalline grains and reduced residual stress over the entire taper waist region.[15] As the SCFs retain a silica cladding, a conventional glass processor workstation (Vytran GPX-3300) could be used for all the tapering processes. The tapered SCFs were then inserted into thicker supporting capillaries before the end facets were polished for optical coupling. In addition to the waist region (L_{waist}), the up- and down-taper transition regions are also retained at each end of the SCF to increase the input and output core sizes (~4.6 μm in diameter) and improve the optical coupling [shown as an inset in Fig. 1(a)]. Two tapered submicrometer SCFs are used in this paper, with their geometrical parameters and total insertion loss summarized in Table S1 (Sec. I in the supplementary material). The input and output tapered regions are normally only a few millimeters long and contribute little to the nonlinear propagation so that one only needs to consider the tapered waist section of the SCF when modeling the nonlinear propagation.

Nonlinear propagation in the tapered SCF waist is governed by the generalized nonlinear Schrödinger equation (NLSE)[16] given as follows:

$$\frac{\partial A(z,t)}{\partial z} + \frac{1}{2}\left(\alpha + \sigma + i\alpha_1 \frac{\partial}{\partial t}\right)A(z,t) - \sum_{n=1}^{\infty} \frac{i^n \beta_n}{n!} \frac{\partial^n A(z,t)}{\partial t^n} = i\left(\gamma + i\gamma_1 \frac{\partial}{\partial t}\right)\left(A(z,t)\int_0^{\infty} R(t')|A(z,t-t')|^2 dt'\right), \quad (1)$$

where $A(z,t)$ is the pulse envelope, β_n is the nth order of dispersion, γ is the nonlinearity parameter, $\gamma_1 = d\gamma/d\omega \approx \gamma/\omega_0$, α is the linear loss, σ is the free carrier parameter, and $\alpha_1 = d\alpha/d\omega$. When expressed in this form, the nonlinear refractive index (n_2) and two-photon absorption (TPA) coefficient (β_{TPA}) contribute to the real and imaginary parts of the nonlinear parameter via $\gamma = k_0 n_2/A_{eff} + i\beta_{TPA}/2A_{eff}$, where A_{eff} is the effective mode area of the tapered waist, and the TPA-induced free carriers give rise to additional loss (σ_f) and dispersion (μ) contributions via $\sigma = \sigma_f(1 + i\mu)N_c$, where N_c is the carrier density. To include Raman effects, both the electronic and vibrational contributions should be included in the nonlinear response function $R(t)$. Assuming that the electronic contribution is nearly instantaneous, the functional form of $R(t)$ can be written as

$$R(t) = (1 - f_R)\delta(t) + f_R h_R(t), \quad (2)$$

where f_R represents the fractional contribution of the delayed Raman response. In silicon, f_R is usually assumed to be 0.043 and $h_R(t)$ can be written in the following form:[17]

$$h_R(t) = \left(\tau_1^{-2} + \tau_2^{-2}\right)\tau_1 \exp(-t/\tau_2)\sin(t/\tau_1), \quad (3)$$

where the phonon lifetime $\tau_1 = 10.256 \times 10^{-3}$ ps and the damping time $\tau_2 = 3.032 \times 10^{-3}$ ps. The remaining parameters are largely fiber specific as they depend on contributions from the core/cladding materials and the waveguide geometry (i.e., core size), and the values estimated for the fibers used in the experiments are given in Table S2 (Sec. II in the supplementary material).[11,14]

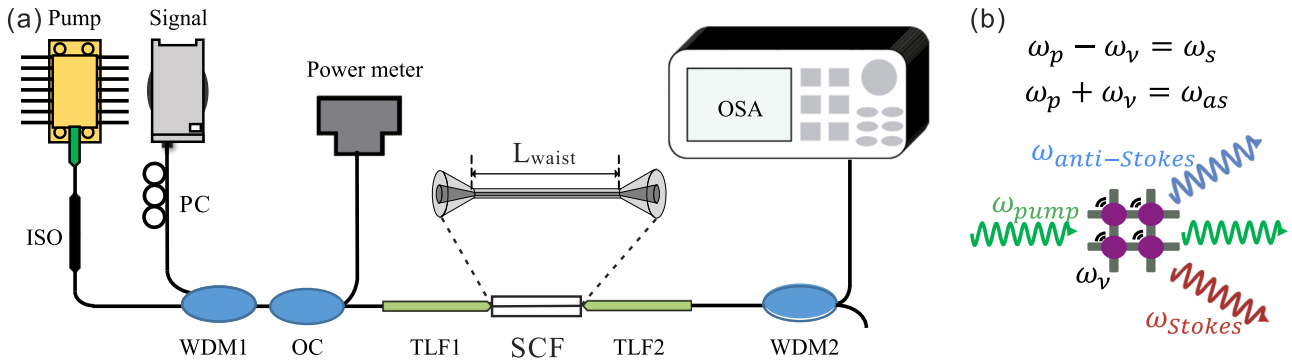

FIG. 1. (a) Schematic of the experimental setup to measure the Raman response of the tapered SCFs. ISO: isolator, PC: polarization controller, WDM: wavelength division multiplexer, OC: optical coupler, TLF: tapered lensed fiber, and OSA: optical spectrum analyzer. The inset shows the geometry for the tapered SCF. (b) Schematic of Raman scattering and energy conservation equations.

III. RESULTS AND DISCUSSION

A. Experimental setup

The experimental setup to characterize the Raman response of the SCFs is shown in Fig. 1(a), together with a schematic of the Raman process and energy conservation equations in Fig. 1(b). For the spontaneous Raman experiments, two CW laser diodes operating at different wavelengths (1431 and 1500 nm) were used as pump sources, with an output power of ~110 mW at these two specific wavelengths. An external isolator was placed after the pump to avoid light reflection into the diode. The pump light was coupled into and out of the SCFs using conventional tapered lensed fibers (TLFs) with a focal diameter of 2.5 μm and a working distance of 14 μm. The TLFs were chosen for the coupling as they have a flat frequency response over the wavelength range covering both the Stokes and anti-Stokes wavelengths. Using the TLF at the input, the pump light could be primarily launched into the fundamental mode of the tapered SCF, which was verified by imaging the output mode profile using a free space lens and CCD, as described in Ref. 16. The optical power was measured using a power meter (Thorlabs S148C), and the output spectra were recorded using an optical spectrum analyzer (OSA—YOKOGAWA AQ6370D) with a resolution of 0.02 nm. To investigate stimulated Raman amplification, a signal laser (TUNICS T100S) was injected into the SCF together with the pump using a wavelength division multiplexer (WDM). A polarization controller (PC) was also used to align the linearly polarized pump and signal beams to optimize the stimulated Raman gain.

B. Spontaneous Raman emission

The SCF used in initial experiments was fabricated to have a tapered waist of 900 nm over a length of L_{waist} = 1 cm, with a total fiber length of ~ 1.4 cm, including the coupling regions. The linear loss at 1550 nm was estimated to be 2.4 dB/cm by subtracting the coupling losses (7 dB) from the total insertion loss (10.2 dB). We note that lower coupling losses could be achieved by fabricating nanospike structures onto the ends of the SCF, which not only helps to better match the mode size with those of the input glass fibers but also reduces reflections.[12] However, fabricating nanospike couplers onto submicrometer core SCFs is challenging due to the small outer dimensions of the tapered fibers, and work in this area is still on-going.

Using the experimental setup, the Stokes spectra were recorded at several values of coupled power for the two different pump wavelengths, as shown in Fig. 2. Forward emitted Stokes signals at (a) 1546.3 nm and (b) 1626.3 nm are generated, which correspond to the Raman shift of 15.6 THz for crystalline silicon in both instances. From Fig. 2, one notes that spontaneous Raman scattering can be clearly observed with a pump power as low as 3 mW and that the Stokes signal power increases with the coupled pump power. The bandwidths of the Stokes signals (263.7 GHz for the 1431 nm pump and 221.2 GHz for the 1500 nm pump) are slightly larger than the theoretical bandwidth of 105 GHz for silicon, which can be attributed to the finite bandwidth of the pump sources.[18] To verify this, the experimental spectra are compared with simulation results that are obtained by convolving the spectra calculated using Eqs. (1)–(3) with the pump laser spectra that are approximated by Gaussian profiles with the linewidths of 146.5 and 102.1 GHz for the

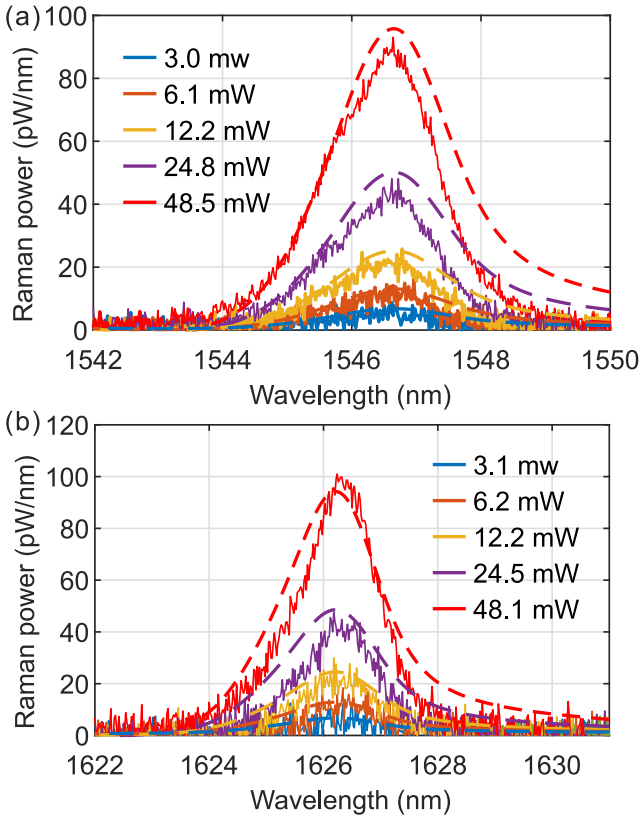

FIG. 2. Spontaneous Raman emission spectra at various pump powers for the pump wavelengths of (a) 1431 nm and (b) 1500 nm.

1431 and 1500 nm pumps, respectively. The agreement between the experiments (solid lines) and simulations (dashed lines) is very good, both in terms of the powers and bandwidths. Moreover, it is worth noting that the maximum recorded Stokes powers were only limited by the available pump laser diode as nonlinear absorption was found to be negligible at these low power levels.

To estimate the Raman gain coefficient of our SCFs, the relationship between the integrated Stokes power and pump power is considered,[19]

$$P_S = \kappa L_{eff} P_p. \quad (4)$$

Here, κ is the spontaneous Raman coefficient in units of cm^{-1} and L_{eff} is the effective length (accounting for the linear losses) of the tapered SCF. Figure 3 plots the integrated Stokes power as a function of coupled power for the two different pump wavelengths. As expected, the spontaneous emission power depends linearly on the pump power, and the slope efficiencies (κL_{eff}) are almost the same for the two pump wavelengths. The spontaneous Raman efficiency S in the SCFs can then be calculated as $S = \kappa/\Delta\Omega$, where $\Delta\Omega$ is the effective solid angle of collection for the fundamental mode, which is estimated to be 0.25 Sr^{-1} for a SCF with an output core diameter of 4.6 μm. Hence, the values of S for the pump wavelengths of 1431 and 1500 nm are 3.03×10^{-7} and 3×10^{-7} $cm^{-1}Sr^{-1}$, respectively. The spontaneous Raman coefficients obtained for these SCFs are similar to previously reported values obtained for nanophotonic silicon

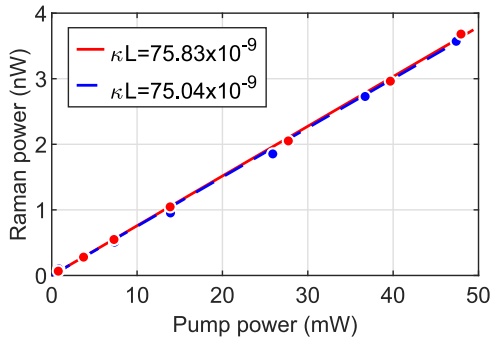

FIG. 3. Spontaneous Raman output power as a function of coupled pump power for the two pump wavelengths of 1431 nm (red) and 1500 nm (blue).

waveguides[19] and are at least two orders of magnitude larger than those of standard silica optical fibers.[1] The Raman gain coefficient g_S is defined using S as[20]

$$g_S = \frac{8\pi c^2 \omega_p}{\hbar \omega_s^4 n^2 (\omega_s)(N+1)\Delta\Omega} S. \tag{5}$$

Here, ω_p and ω_s are the angular frequencies of the pump and Stokes, respectively; n is the refractive index; N is the Bose occupation factor (0.1 at room temperature); $\hbar$ is Planck's constant; and $\Delta\Omega$ is the FWHM bandwidth of the Raman response in silicon. Thus, the values of g_S obtained for the pump wavelengths of 1431 and 1500 nm are 29 and 34 cm/GW, respectively. The consistency of these values is what we would expect for two pumps that are positioned within the telecom band and helps to verify the accuracy of the measurements. Moreover, these g_S values are also consistent with previously reported values obtained for single crystal waveguides, which fall within the range of 20–76 cm/GW.[2,18,21] Thus, these results provide further evidence for the high crystalline material quality of the tapered SCFs.[15]

In addition to the Stokes wave measurements, the anti-Stokes signal was also observed when pumping with coupled powers > 3 mW. Figure 4 shows the Stokes and anti-Stokes spectra obtained with the 1431 nm pump diode for a coupled power of ~ 50 mW, where the anti-Stokes wave is blue shifted from the pump by 15.6 THz. The anti-Stokes spectrum exhibits an asymmetric profile, which we attribute to a combination of the asymmetric linewidth of the pump laser diode and its low power relative to the noise floor. Quantum statistics states that the power ratio between the anti-Stokes (P_{AS}) and Stokes (P_S) waves is defined as[22]

$$\frac{P_{AS}}{P_S} = e^{-h\upsilon_{phonon}/k_B T}, \tag{6}$$

where υ_{phonon} is the phonon frequency, T is the experimental temperature in units of K, and k_B is the Boltzmann constant. The calculated power ratio of 0.08 is in very good agreement with the experimental value of 0.09, which is extracted from the integrated power spectra shown in Fig. 4. With careful design of the fiber dispersion, the generation of the anti-Stokes wave can be dramatically enhanced by coherent anti-Stokes Raman scattering, which has been observed for planar silicon waveguides.[23]

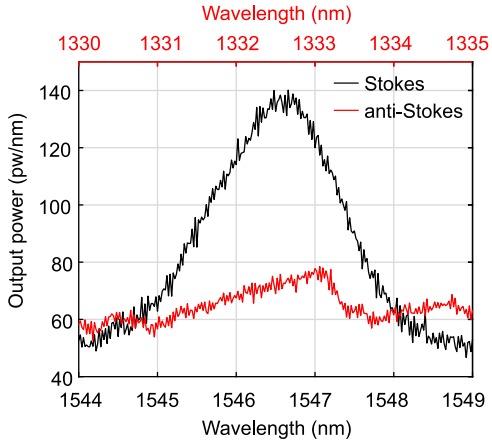

FIG. 4. Comparison of Stokes (bottom wavelength axis) and anti-Stokes (top axis) Raman emission for a pump wavelength of 1431 nm and a coupled power of ~50 mW.

C. Stimulated Raman amplification

Having demonstrated spontaneous Raman emission from the SCF platform, the next step was to investigate its use for Raman amplification. However, as the maximum achievable gain depends on the intensity of the coupled pump and the effective propagation length, for these measurements, a second tapered SCF was fabricated to have a smaller core waist diameter of 750 nm and a length of L_{waist} = 1.5 cm. The total length for this SCF was ~1.9 cm, and the linear loss at 1550 nm was estimated to be 1 dB/cm based on a total insertion loss of 8.9 dB. The experimental setup for stimulated Raman amplification is the same as that shown in Fig. 1(a), but this time the tunable signal laser (TUNICS T100S) was injected into the SCF together with the pump using a WDM. A second WDM positioned at the output stage was used to filter out the noise caused by the pump diode. The signal wavelength was scanned from 1542 to 1550 nm, with the input power fixed to 0.1 mW, and the Stokes power was recorded with the pump on and off. Figure 5 shows the on–off gain curve for a pump power of 48 mW, together with simulation results that are obtained using data from Eqs. (1)–(3) convolved with the pump spectrum. A peak gain of 1.1dB was obtained for a Stokes wavelength of 1546.3 nm, in excellent agreement with the simulations and with the position matched to the spontaneous peak. Additionally, the FWHM linewidth of the gain spectrum is consistent with the simulations and the measured value for spontaneous emission in Fig. 2(a) at a similar pump power. The measured peak Raman gain is slightly larger than what has been reported for sub-micrometer-sized planar silicon waveguides using similar milliwatt level CW pump sources,[2,21] which is attributed to the combination of low fiber transmission loss and longer waveguide length. Moreover, as the measured peak gain was limited by the maximum power of the pump laser diode, there is scope to increase the gain further.

To further probe the Raman performance of the SCFs, additional simulations were conducted to investigate the role of the pump power and fiber length. Figure 6 shows a color map of the on–off gain as functions of the coupled pump power and SCF tapered waist length, assuming that all other parameters (core size,

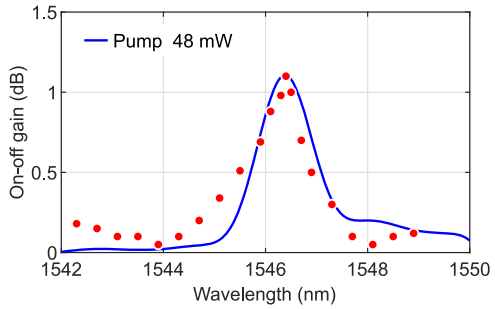

FIG. 5. Stimulated Raman gain for a 1431 nm pump with a coupled power of 48 mW as measured for various signal wavelengths.

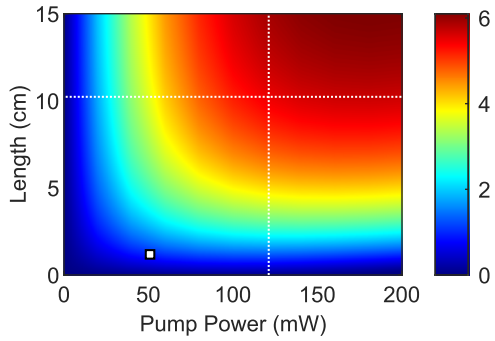

FIG. 6. Simulation results of on–off gain as a function of coupled pump power and SCF tapered waist length. The white square indicates the SCF length and pump power used in the experiment. Dashed lines are a guide to show the maximum stimulated Raman gain.

transmission loss, etc.) remain the same as the fiber described above. The gain estimated for the existing setup matches well with the simulations, as similarly displayed in Fig. 5. These results also show that if the pump power is increased to ~ 120 mW, the maximum gain would increase slightly to 1.6 dB, but that, beyond this, the TPA-induced free carriers become the dominant limitation. Alternatively, if the fiber length could be increased to ~ 10 cm, the gain could reach as high as 6 dB. We note that although this value would be the highest Raman gain obtained for a silicon waveguide system, it would still be considerably less than what has been achieved in highly nonlinear glass fibers.[24] Nevertheless, owing to the high Raman coefficient of the silicon core, SCFs can operate with much lower pump powers (hundreds of mW vs several kW) and shorter lengths (tens of cm vs several km), which is desirable for many practical systems. Currently, the main limitation to fabricating SCFs with such long lengths is the choice of tapering rig, which restricts waist lengths to a few centimeters. However, it has recently been shown that SCFs can be fabricated directly from the drawing tower with losses as low as 0.2 dB/cm over a length of ~ 1 m, albeit for core dimensions of a few micrometers.[25] Assuming that the cores could be reduced to a micrometer, or less, via this approach, these SCFs could be ideal efficient in-fiber Raman amplifiers or lasers operating at modest powers and device lengths.

IV. CONCLUSION

In conclusion, this work has reported the measurements of spontaneous and stimulated Raman scattering generated within SCFs that have been tapered to achieve low propagation losses in submicrometer cores. The Raman gain coefficient of the fibers has been estimated to be $g_s \sim 30$ cm/GW, which is in good agreement with previous measurements in silicon waveguides, further verifying the high crystalline quality of our core material. The peak on–off gain of 1.1 dB is competitive with previous results obtained for planar silicon waveguides with similar dimensions using milliwatt level CW pumping schemes, which is attributed to the low losses and longer fiber lengths. Simulations of the nonlinear propagation suggest that increasing the SCF lengths while retaining small core sizes and low transmission losses is the best way to achieve high Raman gains for the development of all-fiber integrated Raman amplifiers or lasers.

SUPPLEMENTARY MATERIAL

See the supplementary material for the geometrical parameters, insertion losses, and simulation parameters for tapered SCFs.

ACKNOWLEDGMENTS

The authors thank Dr. Sijing Liang, Dr. Lin Xu, and Professor David Richardson for the use of their laser diodes. This publication was supported by the following research funds: the Engineering and Physical Sciences Research Council (EPSRC) (Grant No. EP/P000940/1), the National Natural Science Foundation of China (NSFC) (Grant No. 62175080), the Norwegian Research Council (Grant No. 262232), and the J. E. Sirrine Foundation.

DATA AVAILABILITY

The data that support the findings of this study are openly available in the University of Southampton Institutional Research Repository at https://doi.org/10.5258/SOTON/D1936.

REFERENCES

[1] Y. Aoki, "Properties of fiber Raman amplifiers and their applicability to digital optical communication systems," J. Lightwave Technol. **6**, 1225–1239 (1988).
[2] R. Claps, D. Dimitropoulos, V. Raghunathan, Y. Han, and B. Jalali, "Observation of stimulated Raman amplification in silicon waveguides," Opt. Express **11**, 1731–1739 (2003).
[3] O. Boyraz and B. Jalali, "Demonstration of a silicon Raman laser," Opt. Express **12**, 5269–5273 (2004).
[4] H. Rong, A. Liu, R. Jones, O. Cohen, D. Hak, R. Nicolaescu, A. Fang, and M. Paniccia, "An all-silicon Raman laser," Nature **433**, 292–294 (2005).
[5] Y. Takahashi, Y. Inui, M. Chihara, T. Asano, R. Terawaki, and S. Noda, "A micrometre-scale Raman silicon laser with a microwatt threshold," Nature **498**, 470–474 (2013).
[6] H. Rong, A. Liu, R. Nicolaescu, M. Paniccia, O. Cohen, and D. Hak, "Raman gain and nonlinear optical absorption measurements in a low-loss silicon waveguide," Appl. Phys. Lett. **85**, 2196–2198 (2004).
[7] Q. Xu, V. R. Almeida, and M. Lipson, "Demonstration of high Raman gain in a submicrometer-size silicon-on-insulator waveguide," Opt. Lett. **30**, 35–37 (2005).
[8] L. Shen, H. Ren, M. Huang, D. Wu, and A. C. Peacock, "A review of nonlinear applications in silicon optical fibers from telecom wavelengths into the mid-infrared spectral region," Opt. Commun. **463**, 125437 (2020).

[9]J. Ballato, T. Hawkins, P. Foy, R. Stolen, B. Kokuoz, M. Ellison, C. McMillen, J. Reppert, A. M. Rao, M. Daw, S. Sharma, R. Shori, O. Stafsudd, R. R. Rice, and D. R. Powers, "Silicon optical fiber," Opt. Express **16**, 18675–18683 (2008).
[10]E. F. Nordstrand, A. N. Dibbs, A. J. Eraker, and U. J. Gibson, "Alkaline oxide interface modifiers for silicon fiber production," Opt. Mater. Express **3**, 651–657 (2013).
[11]F. H. Suhailin, L. Shen, N. Healy, L. Xiao, M. Jones, T. Hawkins, J. Ballato, U. J. Gibson, and A. C. Peacock, "Tapered polysilicon core fibers for nonlinear photonics," Opt. Lett. **41**, 1360–1363 (2016).
[12]H. Ren, O. Aktas, Y. Franz, A. F. J. Runge, T. Hawkins, J. Ballato, U. J. Gibson, and A. C. Peacock, "Tapered silicon core fibers with nano-spikes for optical coupling via spliced silica fibers," Opt. Express **25**, 24157–24163 (2017).
[13]R. Sohanpal, H. Ren, L. Shen, C. Deakin, A. M. Heidt, T. W. Hawkins, J. Ballato, U. J. Gibson, A. C. Peacock, and Z. Liu, "Parametric frequency comb generation using silicon core fiber," in 2021 Optical Fiber Communication Conference (OFC), 2021.
[14]D. Wu, L. Shen, H. Ren, M. Huang, C. Lacava, J. Campling, S. Sun, T. W. Hawkins, U. J. Gibson, P. Petropoulos, J. Ballato, and A. C. Peacock, "Four-wave mixing-based wavelength conversion and parametric amplification in submicron silicon core fibers," IEEE J. Sel. Top. Quantum Electron. **27**, 4300111 (2021).
[15]Y. Franz, A. F. J. Runge, H. Ren, N. Healy, K. Ignatyev, M. Jones, T. Hawkins, J. Ballato, U. J. Gibson, and A. C. Peacock, "Material properties of tapered crystalline silicon core fibers," Opt. Mater. Express **7**, 2055–2061 (2017).
[16]H. Ren, L. Shen, D. Wu, O. Aktas, T. Hawkins, J. Ballato, U. J. Gibson, and A. C. Peacock, "Nonlinear optical properties of polycrystalline silicon core fibers from telecom wavelengths into the mid-infrared spectral region," Opt. Mater. Express **9**, 1271–1279 (2019).
[17]Q. Lin, O. J. Painter, and G. P. Agrawal, "Nonlinear optical phenomena in silicon waveguides: Modeling and applications," Opt. Express **15**, 16604–16644 (2007).
[18]R. Claps, D. Dimitropoulos, Y. Han, and B. Jalali, "Observation of Raman emission in silicon waveguides at 1.54 μm," Opt. Express **10**, 1305–1313 (2002).
[19]J. I. Dadap, R. L. Espinola, R. M. Osgood, S. J. McNab, and Y. A. Vlasov, "Spontaneous Raman scattering in ultrasmall silicon waveguides," Opt. Lett. **29**, 2755–2757 (2004).
[20]J. M. Ralston and R. K. Chang, "Spontaneous-Raman-scattering efficiency and stimulated scattering in silicon," Phys. Rev. B **2**, 1858–1862 (1970).
[21]R. L. Espinola, J. I. Dadap, R. M. Osgood, S. J. McNab, and Y. A. Vlasov, "Raman amplification in ultrasmall silicon-on-insulator wire waveguides," Opt. Express **12**, 3713–3718 (2004).
[22]B. Jalali, V. Raghunathan, D. Dimitropoulos, and O. Boyraz, "Raman-based silicon photonics," IEEE J. Sel. Top. Quantum Electron. **12**, 412–421 (2006).
[23]R. Claps, V. Raghunathan, D. Dimitropoulos, and B. Jalali, "Anti-Stokes Raman conversion in silicon waveguides," Opt. Express **11**, 2862–2872 (2003).
[24]S. Liang, S. Jain, L. Xu, K. R. H. Bottrill, N. Taengnoi, M. Guasoni, P. Zhang, M. Xiao, Q. Kang, Y. Jung, P. Petropoulos, and D. J. Richardson, "High gain, low noise, spectral-gain-controlled, broadband lumped fiber Raman amplifier," J. Lightwave Technol. **39**, 1458–1463 (2021).
[25]M. Kudinova, G. Bouwmans, O. Vanvincq, R. Habert, S. Plus, R. Bernard, K. Baudelle, A. Cassez, B. Chazallon, M. Marinova, N. Nuns, and L. Bigot, "Two-step manufacturing of hundreds of meter-long silicon micrometer-size core optical fibers with less than 0.2 dB/cm background losses," APL Photonics **6**, 026101 (2021).